Journal of Cerebral Blood Flow & Metabolism (2011) 31, 725–737

www.jcbfm.com

Noninvasive and localized blood–brain barrier disruption using focused ultrasound can be achieved at short pulse lengths and low pulse repetition frequencies

James J Choi[1], Kirsten Selert[1], Zimeng Gao[1], Gesthimani Samiotaki[1], Babak Baseri[1] and Elisa E Konofagou[1,2]

[1]*Department of Biomedical Engineering, Columbia University, New York, New York, USA;* [2]*Department of Radiology, Columbia University, New York, New York, USA*

Ultrasound methods in conjunction with microbubbles have been used for brain drug delivery, treatment of stroke, and imaging of cerebral blood flow. Despite advances in these areas, questions remain regarding the range of ultrasound parameters that disrupt the blood–brain barrier (BBB). In this study, several conditions were investigated to either enhance or reduce the likelihood of BBB disruption. Pulsed focused ultrasound (frequency: 1.5 MHz, pressure: 0.46 MPa, pulse repetition frequency (PRF): 0.1 to 25 Hz, pulse length (PL): 0.03 to 30 milliseconds) was noninvasively and locally administered to a predetermined region in the left hemisphere in the presence of circulating preformed microbubbles (Definity, Lantheus Medical Imaging, N. Billerica, MA, USA; 0.01, 0.05, 0.25 μL/g). Trans-BBB delivery of 3-kDa dextran was observed at PRFs as low as 1 Hz, whereas consistent delivery was observed at 5 Hz and above. Delivery was demonstrated at a PL as low as 33 microseconds. Although the delivered dextran concentration increased with the PL, this also increased the heterogeneity of the resulting distribution. In conclusion, key parameters that disrupt the BBB were identified out of a wide range of conditions. Reducing the total number of emitted acoustic cycles by shortening the PL, or decreasing the PRF, was also found to facilitate a more spatially uniform distribution of delivered dextran.
Journal of Cerebral Blood Flow & Metabolism (2011) **31,** 725–737; doi:10.1038/jcbfm.2010.155; published online 15 September 2010

Keywords: blood–brain barrier; brain drug delivery; dextran; focused ultrasound; microbubbles

Introduction

Noninvasive ultrasound techniques in conjunction with microbubble have been reported for the treatment and diagnosis of several central nervous system and cerebrovascular diseases. These methods include sonothrombolysis for the treatment of stroke (Datta *et al*, 2008; Meairs and Culp, 2009), Doppler imaging of cerebral blood flow (Meyer-Wiethe *et al*, 2009; Tsivgoulis *et al*, 2009), and blood–brain barrier (BBB) disruption for the delivery of pharmacological agents (Choi *et al*, 2007*b*, 2010*b*; Hynynen *et al*, 2001). Typically, preformed, lipid- or polymer-shelled microbubbles ($<10\,\mu$m in diameter) are first systemically administered. The brain is then exposed to ultrasonic pulses, which activate the microbubbles within the cerebral vasculature in an array of behaviors that can range from stable oscillations to unstable collapse (Borden *et al*, 2005). The type of acoustically driven microbubble activity, or acoustic cavitation, is dictated by the microbubble design and distribution, the ultrasonic pulse shape and sequence, and the heterogeneous cerebral vasculature, in which microbubbles circulate. Thus, selected parameters are critical in generating distinct cerebrovascular responses necessary for effective and safe brain therapeutic and diagnostic methods (Chomas *et al*, 2001; Tsivgoulis and Alexandrov, 2007).

A key indicator of altered cerebrovascular physiology is disruption of the BBB, which is detectable by the deposition of normally BBB-impermeable agents in the brain parenchyma. In the cases of cerebral blood flow imaging and sonothrombolysis, this effect is undesirable and acoustic and microbubble conditions should be selected to avoid its occurrence (Tsivgoulis and Alexandrov, 2007). However, this

Correspondence: Dr EE Konofagou, Department of Biomedical Engineering, Columbia University, 351 Engineering Terrace, mail code 8904, 1210 Amsterdam Avenue, New York, NY 10027 USA.
E-mail: ek2191@columbia.edu
This study was supported by the National Institutes of Health (R01 EB 009041 and R21EY 018505), National Science Foundation (CAREER 0644713), and Kinetics Foundation.
Received 31 March 2010; revised 27 July 2010; accepted 28 July 2010; published online 15 September 2010

same phenomenon is essential to the development of a brain drug delivery system. Ultrasound-induced BBB disruption has shown promise due to its ability to deliver large therapeutic agents to a targeted brain volume on the order of millimeters (Choi *et al*, 2010*b*; Kinoshita *et al*, 2006). Focused ultrasound (FUS) entails acoustic waves that can noninvasively propagate to deep subcortical structures through the intact scalp and skull. As the acoustically driven microbubbles act on the cerebral vasculature, the extensive capillary network is used to help deliver the molecules, e.g., large therapeutic agents such as Herceptin (Kinoshita *et al*, 2006) and Doxorubicin (Treat *et al*, 2007). Hematoxylin and eosin (H&E)-stained sections have shown that BBB disruption can be induced without neuronal damage or erythrocyte extravasations (Baseri *et al*, 2010). Despite the many advances to the development of this technology, several concerns remain including the spatial distribution and concentration of the agents delivered, the mechanism of disruption, and the suitability of parameters for use in a clinical system. Fundamentally, the rationale for using the ultrasound and microbubble conditions previously reported by our group and others remains unknown.

The purpose of this study is to investigate a wide range of ultrasound and microbubble conditions *in vivo* for their ability to disrupt the BBB. In mouse experiments, we will reveal parameters that are critical for inducing BBB disruption as well as parameters that avoid or reduce the extent of BBB disruption. Our investigation will include several key conditions: sonication duration, microbubble concentration, pulse repetition frequency (PRF), and pulse length (PL). Ultimately, we will show that a larger range of parameters may be used to disrupt the BBB and that the consistency and spatial distribution of molecular delivery can be enhanced.

Materials and methods

Animals

A total of 99 C57Bl6 male mice (24.71 ± 1.77 g; Harlan Laboratories, Indianapolis, IN, USA) were used. Each mouse was anesthetized with a mixture of oxygen (0.8 L/min at 1.0 Bar, 21°C) and 1.5% to 2.0% vaporized isoflurane (Aerrane, Baxter Healthcare, Deerfield, IL, USA) using an anesthesia vaporizer (SurgiVet, Smiths Group, Waukesha, WI, USA). The mouse's respiration rate was monitored and isoflurane was adjusted throughout the experiments as needed. The Columbia University Institutional Animal Care and Use Committee approved all mouse studies presented.

Ultrasound Equipment and Targeting Procedure

A single-element, spherical-segment FUS transducer (center frequency: 1.525 MHz, focal depth: 90 mm, radius: 30 mm; Riverside Research Institute, New York, NY, USA) was driven by a function generator (Agilent, Palo Alto, CA, USA) through a 50-dB power amplifier (E&I, Rochester, NY, USA). A pulse-echo transducer (center frequency: 7.5 MHz; focal length 60 mm) was used in our brain targeting system and was positioned through a central, circular hole of the FUS transducer so that their foci were aligned. The targeting transducer was driven by a pulser-receiver system (Olympus, Waltham, MA, USA) connected to a digitizer (Gage Applied Technologies, Inc., Lachine, QC, Canada). A cone-shaped chamber, which was mounted on the transducer system, was filled with degassed and distilled water and enclosed with an acoustically transparent latex membrane (Trojan; Church & Dwight Co., Inc., Princeton, NJ, USA) (Figure 1). The transducers were attached to a computer-controlled, three-dimensional positioning system (Velmex Inc., Lachine, QC, Canada).

The details of the FUS transducer's acoustic pressure amplitude and beam profile measurements were reported elsewhere (Choi *et al*, 2007*a*, *b*). In brief, the peak-rarefactional pressure amplitudes reported in this study were measured with a needle hydrophone (needle diameter: 0.2 mm; Precision Acoustics Ltd., Dorchester, Dorset, UK) in degassed water while accounting for 18% attenuation through the parietal bone of the mouse skull. The lateral and axial full width at half maximum intensity was measured to be $\sim$1.3 and 13.0 mm, respectively.

The mouse head was immobilized using a stereotactic apparatus. The fur on top of the head was removed with an electric razor and a depilatory cream. After applying ultrasound coupling gel (Aquasonic, Parker Laboratories, Inc., Fairfield, NJ, USA), a water container with its bottom made of an acoustically and optically transparent membrane was placed on top of the head and gel. A grid positioning method to target the region of interest (ROI), which corresponded to the left hippocampus and lateral portion of the thalamus (Figure 1B), was then used as previously described (Choi *et al*, 2007*b*). In brief, a metallic grid was aligned with specific skull sutures, which were visible through the skin, and then imaged using the pulse-echo transducer in a raster scan. The transducers were moved 2.5 mm lateral of the sagittal suture and 2.0 mm anterior of the lambdoid suture so that its focus overlapped with the target ROI. This targeting method was capable of placing the peak of the FUS beam within 1 mm of the intended target. The right hemisphere was not targeted and acted as the control.

Microbubble and Dextran Formulation

Lysine-fixable dextran was fluorescently tagged with Texas Red (Invitrogen, Carlsbad, CA, USA) and was used as the model drug. The dextran was selected to be 3-kDa in molecular weight as it is above the 400-Da threshold that can penetrate the BBB while remaining larger than several therapeutic molecules that have been effective *in vitro*, but cannot traverse the BBB. For example, β-secretase inhibitors ($\sim$1.6 kDa) and brain-derived neurotrophic factor (BDNF) mimetics ($\sim$1.2 kDa) are BBB impermeable but otherwise promising for the treatment of Alzheimer's and Parkinson's disease, respectively. Dextran was dissolved in phosphate-buffered saline and Definity (USA; diameter: 1.1 to 3.3 μm,

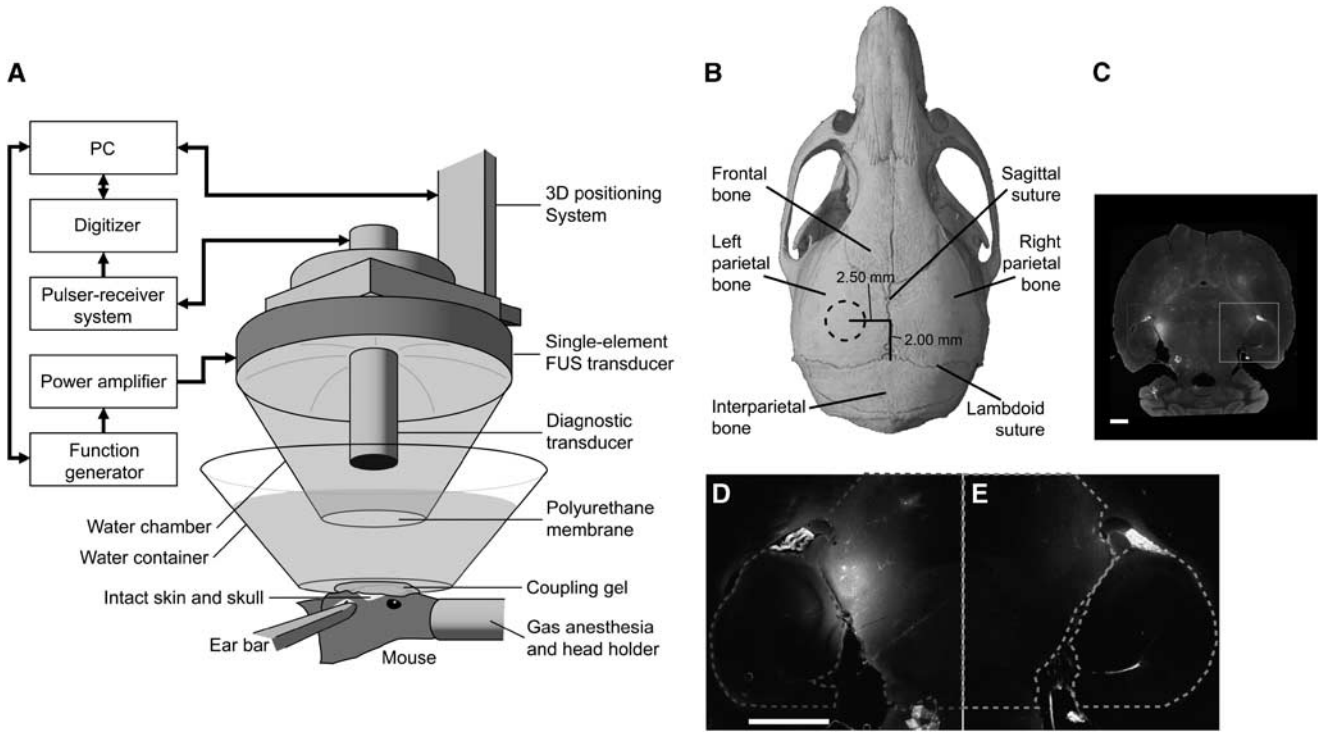

Figure 1 (**A**) *In vivo* focused ultrasound (FUS)-induced blood–brain barrier (BBB) opening experimental setup. The FUS transducer was targeted through (**B**) the left parietal bone of the mouse skull. The dotted circle in (**B**) approximately corresponds to the diameter of the focus within the region outlined in (**C**) (blue solid). Both the left (blue solid) and right (red solid) regions of interest (ROIs) were then outlined as in (**D**, **E**), respectively. The fluorescence within each ROI was normalized to the right hippocampus, thresholded, and the fluorescence values were then summed to obtain a normalized optical density (NOD) value. The color reproduction of this figure is available on the html full text version of the manuscript.

vial concentration: 1.2×10^{10} bubbles/mL; Lantheus Medical Imaging, N. Billerica, MA, USA), composed of octafluoropropane gas encapsulated in a lipid shell, were mixed into the solution. Then, 100 μL of the solution was injected into the tail vein (dextran concentration: 60 μg/g of body mass) during 30 seconds either before or after sonication, depending on the experimental protocol.

Experimental Conditions

The left ROI was exposed to one of the 18 distinct experimental conditions (Table 1), whereas the right remained unsonicated (Figure 1). In one of the conditions, mice underwent a sham whereby the protocol remained identical except there was no sonication. In all other 17 conditions, a 1.525-MHz acoustic beam at a peak-rarefactional pressure of 0.46 MPa was used.

The delivery protocol consisted of intravenous injection of the microbubble and dextran formulation either 1 minute before a 30-second sonication or 1 minute after the start of an 11-minute sonication. The 30-second sonication protocol was similar to what was used in our previous study, whereas the 11-minute sonication protocol was used to accentuate the BBB disruption so that subtle differences among the experimental conditions could be evaluated.

Unless otherwise noted, all subsequent conditions consisted of sonications according to the 11-minute protocol with a 20-millisecond PL and a 10-Hz PRF, and microbubble injections over a 30-second duration and at a 0.05 μL/g concentration. The influence of microbubble concentration was evaluated at the clinically recommended contrast agent dosage used for human echocardiography (0.01 μL/g of body mass) and at higher dosages (0.05 and 0.25 μL/g). Concentrations above the recommended diagnostic limit were explored here to determine whether they accentuated the BBB disruption, and thus could be used to detect subtle differences among the experimental conditions. The PRF was evaluated at 0.1, 1, 5, 10, and 25 Hz, which corresponded to pulse repetition periods of 10, 1, 0.2, 0.1, and 0.04 seconds, respectively. The PL was evaluated at 0.033, 0.1, 0.2, 1, 2, 10, 20, and 30 milliseconds, which corresponded to 50, 152, 304, 1520, 3,040, 15,200, 30,400, and 45,600 acoustic cycles, respectively. Finally, the lowest PRF and PL that resulted in dextran delivery were combined and used in a single FUS sonication. Sonications were applied with a 0.2-millisecond PL and a 5-Hz PRF, and microbubbles were administered over the course of 30 or 180 seconds.

Brain Preparation

Approximately 20 minutes after administration of the combined microbubble and dextran formulation, the mice were transcardially perfused with 30 mL of phosphate-buffered

Table 1 Summary of the 18 experimental conditions

Microbubble concentration (μL/g of body mass)	*Pulse repetition frequency (Hz)*	*Pulse length (milli-seconds)*	*Normalized optical density (mean ± s.d.) × 1e9*	*Number of mice with delivered dextran*
0.05[a]	—	—	0.01 ± 0.23	0 out of 5
0.05[b]	10	20	4.91 ± 0.94	5 out of 5
0.05	10	20	4.45 ± 2.08	5 out of 5
0.01	10	20	2.89 ± 1.99	5 out of 5
0.25	10	20	5.34 ± 2.12	5 out of 5
0.05	0.1	20	−0.17 ± 0.17	0 out of 5
0.05	1	20	3.77 ± 4.52	3 out of 5
0.05	5	20	4.21 ± 2.05	5 out of 5
0.05	25	20	4.58 ± 1.40	5 out of 5
0.05	10	0.03	0.78 ± 1.41	2 out of 5
0.05	10	0.1	1.20 ± 1.05	5 out of 6
0.05	10	0.2	0.98 ± 0.67	5 out of 5
0.05	10	1	4.07 ± 3.71	5 out of 5
0.05	10	2	1.84 ± 1.44	4 out of 5
0.05	10	10	4.76 ± 2.03	5 out of 5
0.05	10	30	5.77 ± 1.73	5 out of 5
0.05	5	0.2	2.02 ± 1.38	5 out of 5
0.05[c]	5	0.2	1.58 ± 1.37	5 out of 5

In 16 conditions, mice were intravenously injected with a solution of dextran and microbubbles 1 minute after the start of an 11-minute sonication. The other two conditions consisted of a sham (no ultrasound) and a protocol, where the solution was intravenously administered 1 minute before a 30-second sonication. Microbubbles were administered over a duration of 30 seconds under all conditions except one where a 180-second duration was used.

[a]Sham mouse. No ultrasound was applied.

[b]Microbubble and dextran were administered 1 minute before a 30-second sonication.

[c]Microbubbles were injected over 180 seconds.

saline (138 mmol/L sodium chloride, 10 mmol/L phosphate, pH 7.4) and 60 mL of 4% paraformaldehyde. This corresponded to perfusion being initiated 21 minutes after the start of the 11-minute sonication protocol and 19 minutes after the start of the 30-second sonication protocol. The brain, which remained encased in the skull was soaked in 4% paraformaldehyde, extracted from the skull the next day, and separately soaked in 4% paraformaldehyde for an additional day. Ninety-one of the brains were then prepared for fluorescence microscopy and image analysis. Another five brains that were exposed to acoustic parameters near the threshold of BBB disruption and three control mice not exposed to FUS were prepared for paraffin embedding, sectioning, and H&E staining.

Brains were prepared for fluorescence microscopy by serial dilution of 10%, 20%, and then 30% sucrose at 30 minutes, 1 hour, and overnight time increments, respectively. They were then embedded in a formulation of water-soluble glycols and resins (Sakura Tissue-Tek O.C.T. Compound; Torrance, CA, USA), frozen in a square mold, and then sectioned using a cryostat into 100-μm slices in the horizontal orientation. Images of all frozen sections were then acquired using an upright fluorescence microscope (BX61; Olympus, Melville, NY, USA). The entire horizontal section was imaged at $\times 12.5$ magnification, whereas the left and right ROIs were separately imaged at $\times 40$ magnification. The Texas Red-tagged dextran was excited at 568 ± 24 nm, whereas emissions were filtered for 610 ± 40 nm.

Brains were prepared for H&E staining using standard paraffin embedding and sectioning procedures. Specimens were horizontally sectioned into 6-μm-thick slices in 12 separate levels that covered the entire hippocampus. First, a 1.2-mm layer was trimmed away from the dorsal brain and discarded. Six sections were serially sectioned, and then another 80 μm of tissue was discarded. The process was repeated for another 11 levels, totaling 72 collected sections. At each level, the first two sections were H&E stained, whereas the rest remained unstained. Bright field microscopy of the H&E-stained sections was used to assess damage, whereas fluorescence microscopy of the unstained sections was used to confirm successful dextran delivery. Both examinations for damage and image acquisitions were performed using the bright field and fluorescence microscopy.

Fluorescence Microscopic Examination of Dextran Delivery

The number of sections analyzed for each brain was narrowed down to nine. A section representing the ventral-dorsal midline was selected as determined by anatomical landmarks. Four dorsal and four ventral sections to this midline were then selected. If a section had preparation or sectioning artifacts (e.g., separation of the hippocampus from the thalamus, overlapping brain tissue because of folding, etc.), it was excluded from analysis and a neighboring section was selected. The FUS-targeted (left) and control (right) ROI of a section were defined as their respective hippocampal and thalamic regions (Figure 1). For every section analyzed, ROIs were manually outlined using Adobe Photoshop CS3 (San Jose, CA, USA) and used to quantify the extent of dextran delivery.

The fluorescence images were processed to quantify: (1) a normalized optical density (NOD) value that represented a relative increase in the amount of dextran delivered to the target ROI and (2) the probability of dextran delivery occurring given an experimental condition. Every fluorescence image was normalized by dividing each image by the spatial average of the right (control) hippocampus as determined using the outlines (Figure 1). Fluorescence pixel intensities because of dextran delivery were separated from background brain autofluorescence by applying a threshold on each image section. This threshold was defined as a fluorescence intensity of twice the s.d. of the right (control) hippocampus. All fluorescence pixels were then summed in their respective hemispheric ROIs for all sections of a given brain. The left hemispheric summation value was then subtracted by its contralateral right hemispheric value to provide the NOD value. For each brain, the NOD thus approximated the sum of all pixels with fluorescence above the set threshold that indicated delivery of dextran. A NOD value for each of the 18 experimental conditions was then obtained by averaging the NOD of all mice exposed under specific conditions (Table 1).

Successful *in vivo* dextran delivery for an individual brain was concluded if the NOD was higher by at least

1 s.d. relative to the average of the sham experimental condition. The probability of dextran delivery was then calculated as being equal to the number of mouse brains exposed to a given experimental condition yielding successful delivery divided by the total number of mouse brains exposed.

Bright Field Microscopic Examination of Damage

The H&E-stained sections were microscopically examined for tissue damage as indicated by dark neurons, microvacuolations, and erythrocyte extravasation sites. Damaged neurons were identified based on characteristics of dark neurons, which had shrunken and triangulated cell bodies, eosinophilic perikaryal cytoplasm, and pyknotic basophilic nuclei. Microvaculations of brain parenchyma were visualized and recorded as apparent voids in the section. An erythrocyte extravasation site was identified as a cluster of five or more erythrocytes. The right ROI acted as the control region in every mouse evaluated for damage. The general appearance of the control ROI was taken into account when the left ROI was analyzed microscopically, accounting for any artifacts or general poor tissue quality that could have occurred because of inadequate fixation, poor tissue handling or processing, or the experimental procedure itself. Additional measures were incorporated to avoid the 'dark neuron artifact' caused by postmortem trauma as a result of inadequate perfusion fixation or improper tissue handling (Cammermeyer, 1960, 1978). Safety analysis was performed by a single trained observer.

In the case of each brain, eight sections corresponding to eight different levels showing the greatest amount of damage were selected (covering 0.85 mm of hippocampus) and three histological measures were evaluated. The total number of dark neurons, microvacuolations, and erythrocyte extravasation sites were calculated for the left (sonicated) and right (control) ROIs in each section. The values for each histological measure obtained from the eight sections were summed at their respective brain hemispheres, and the net difference was calculated by subtracting the right ROI values from those in the left ROI. The net difference values were then averaged across all brains exposed to the same experimental conditions and s.d. values were obtained.

Statistical Analysis

Differences between the two sets of values were determined using statistical analysis. Following the calculation of the mean and s.d. in NOD or histological measure, a two-sided Student's *t*-test was performed. In all comparisons, a difference in fluorescence at $P<0.05$ was considered statistically significant.

Results

In the sham mice, in which no FUS was applied, no difference in fluorescence was observed between the two hemispheres (Figures 2A and 2B). This was confirmed quantitatively as no significant NOD difference between the left (FUS targeted) and right (control) ROIs was calculated. The NOD of 17 distinct experimental conditions were compared with this sham to determine whether significant NOD increase were observed, i.e., whether dextran was sufficiently delivered.

Sonication Duration

Both the 30-second and 11-minute sonication protocols delivered dextran to the left ROI (Figures 1B–1D) using a 1.525-MHz acoustic wave at 0.46 MPa, a 10-Hz PRF, and a 20-millisecond PL (Table 1). The dextran distribution was (1) diffuse throughout certain regions within the larger target volume and (2) contained within or near large vessels (i.e., posterior cerebral artery, longitudinal hippocampal vessels) and their immediate branches (Figures 2C and 2E). The NOD was significantly higher than the sham mice for both protocols (Figure 2K) and dextran delivery was observed in all mice evaluated (10 out of 10), thus, indicating consistency of delivery. Comparison of the 30-second and 11-minute sonication protocols revealed neither a significant difference in NOD nor a difference in the distribution characteristics.

Microbubble Concentration

At each microbubble concentration of 0.01, 0.05, and 0.25 μL/g of body mass, dextran was delivered to the target ROI (Figures 1B–1D). These conditions followed the 11-minute sonication protocol and used a 1.525-MHz acoustic beam at 0.46 MPa, a 20-millisecond PL and a 10-Hz PRF (Table 1). Dextran distribution was both diffuse and contained within or near large vessels (Figures 2E, 2G, and 2I), as similarly observed with the 30-second sonication protocol. The NOD increases were significant at each microbubble concentration evaluated (Figure 2L), and dextran was delivered in every mouse in this study (15 out of 15). However, comparison among the three concentrations revealed neither a significant difference in NOD nor a difference in the dextran distribution characteristics.

Pulse Repetition Frequency

The PRFs of 0.1, 1, 5, 10, and 25 Hz were evaluated regarding their ability to deliver dextran. No dextran delivery was observed at 0.1-Hz PRF (Figure 3A), and this was confirmed as an insignificant difference relative to the sham (Figure 3K). Less consistent results were observed at 1-Hz PRF. Figure 3C depicts a spatial distribution that is representative of the middle of the two extremes of very high fluorescence and no detectable fluorescence. Assessment of characteristic spatial distributions at 1-Hz PRF were

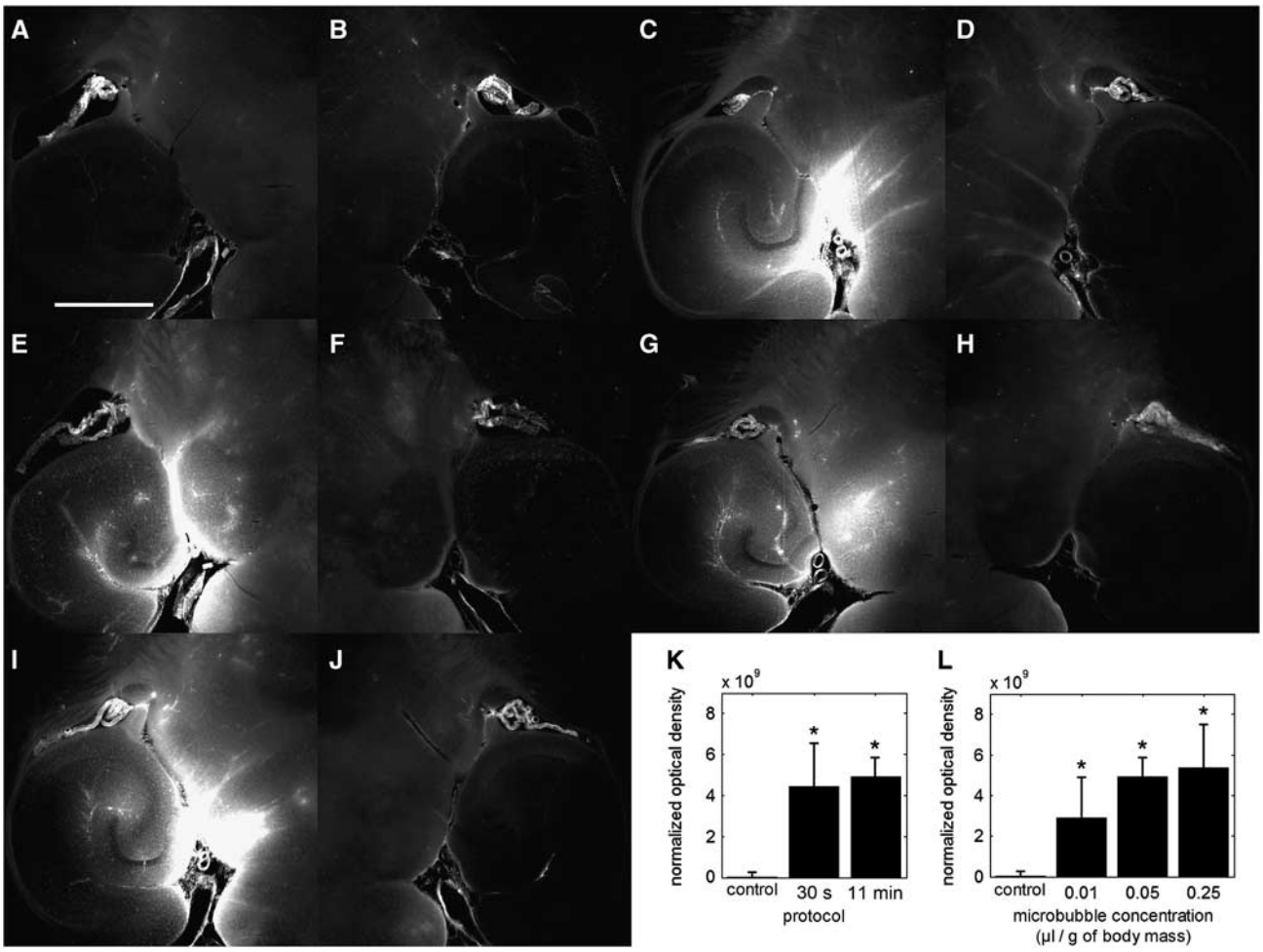

Figure 2 Qualitative fluorescence images of the (**A**, **C**, **E**, **G**, **I**) left and (**B**, **D**, **F**, **H**, **J**) right brain regions of interest (ROI) that have been exposed to different protocols and microbubble concentrations. No detectable difference in fluorescence was observed between the left and right ROIs of (**A**, **B**) a control mouse that was not sonicated. However, fluorescence increases in the (**C**, **E**, **G**, **I**) focused ultrasound (FUS)-targeted left ROIs was clearly observed when compared with the (**D**, **F**, **H**, **J**) control (right) ROIs. Sonication of the left ROI in (**C**) was performed according to the 30-second protocol, whereas sonication of left ROI in (**E**, **G**, **I**) was performed according to the 11-minute protocol. Microbubble concentrations were set to (**C**, **E**) 0.05, (**G**) 0.01, and (**J**) 0.25 μL/g of body mass. The white scale bar in (**A**) indicates 1 mm. Quantitative normalized optical density (NOD) values of the left ROI that was exposed to different (**K**) sonication protocols and (**L**) microbubble concentrations. The NOD values were calculated relative to the right (nonsonicated) ROI. (**K**) Both the 30-second and 11-minute sonication protocols used a microbubble concentration of 0.05 μL/g of body mass and (*) significant increases in NOD were observed relative to the sham ($P < 0.05$). (**L**) Microbubble concentrations of 0.01, 0.05, and 0.25 μL/g of body mass while using the 11-minute sonication protocol induced significant levels of NOD increase.

difficult due to the fluorescence variability. Only 60% of the mice (3 out of 5) exhibited delivery (Figure 3L), and the NOD increase was not significant. At 5, 10, and 25 Hz PRFs, large concentrations of dextran were delivered in both diffuse and contained regions (Figures 3E, 3G, and 3I). The NOD increases were significant relative to the sham and consistent in all mice evaluated (15 out of 15; Figures 3K and 3L). However, comparison among different PRF cases (5, 10, and 25 Hz) revealed no significant difference in NOD, thus indicating that, beyond a certain PRF, a higher concentration of dextran may not be delivered.

Pulse Length

The PLs of 0.033, 0.1, 0.2, 1.0, 2.0, 10, 20, and 30 milliseconds were evaluated regarding their ability to deliver dextran. The lowest PL whereby dextrans were delivered was at 0.033 milliseconds (Figure 4A), which was observed in two out of five mice evaluated (Figure 4R). The lowest PL, at which a significant NOD increase was observed, was 0.1 millisecond, and the lowest PL, at which every mouse exhibited a detectable level of NOD, was at 0.2 milliseconds (Figures 4Q and 4R). At each PL of 0.033, 0.1, and 0.2 milliseconds, dextran was

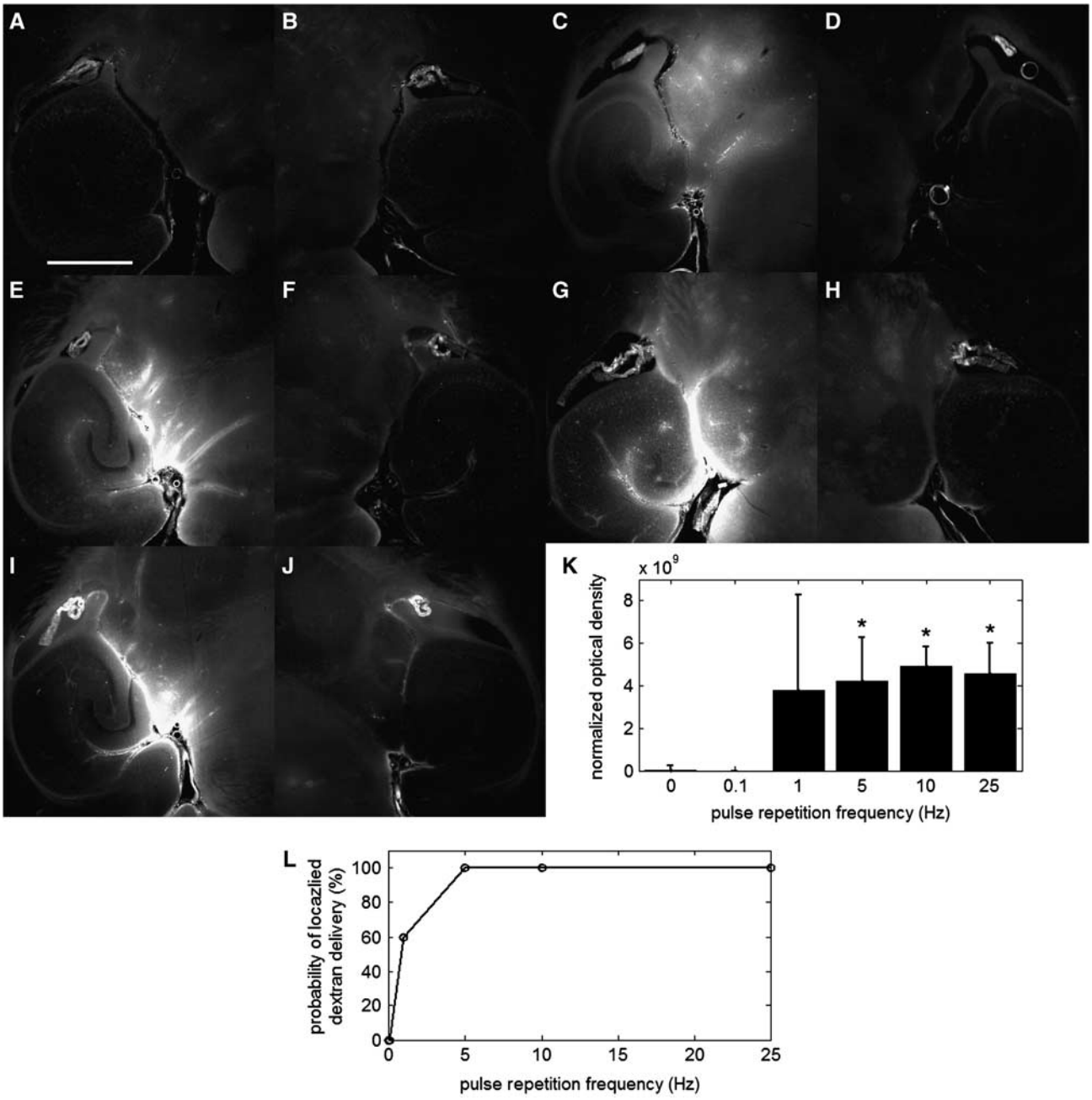

Figure 3 Qualitative fluorescence images of the left (**A**, **C**, **E**, **G**, **I**) and right (**B**, **D**, **F**, **H**, **J**) brain regions of interest (ROI) that have been exposed to different pulse repetition frequencies (PRFs). No detectable difference in fluorescence was observed between the left and right ROIs of (**A**, **B**) a mouse sonicated at a PRF of 0.1 Hz. Detectable differences compared with the sham were observed at PRFs of (**C**) 1, (**E**) 5, (**G**) 10, and (**I**) 25 Hz. The white scale bar in (**A**) indicates 1 mm. Quantitative (**K**) normalized optical density (NOD) values of the left focused ultrasound (FUS)-targeted ROI and (**L**) probability of localized dextran delivery. The left ROI was sonicated with PRFs of 0.1, 1, 5, 10, and 25 Hz. The asterisk (*) indicates a significant increase in NOD relative to the sham ($P < 0.05$).

distributed diffusely throughout the region, although containment within vessels was also observed in some cases (Figures 4A, 4C, and 4E). All PLs beyond 0.2 milliseconds exhibited significant NOD increases compared to the sham case, and consistently delivered dextran (Figures 4Q and 4R) with the exception of the 2-millisecond PL case, where one out of five mice tested did not produce a detectable level of fluorescence. The dextran was both diffusely distributed in some regions and contained within or near vessels (Figures 4G, 4I, 4K, 4M, and 4O). Fluorescence at or near vessels was particular prominent at PLs of 10, 20, and 30 milliseconds.

Comparisons of NOD levels among the different PL conditions yielded interesting findings. The NOD levels between 0.1 and 0.2 milliseconds were

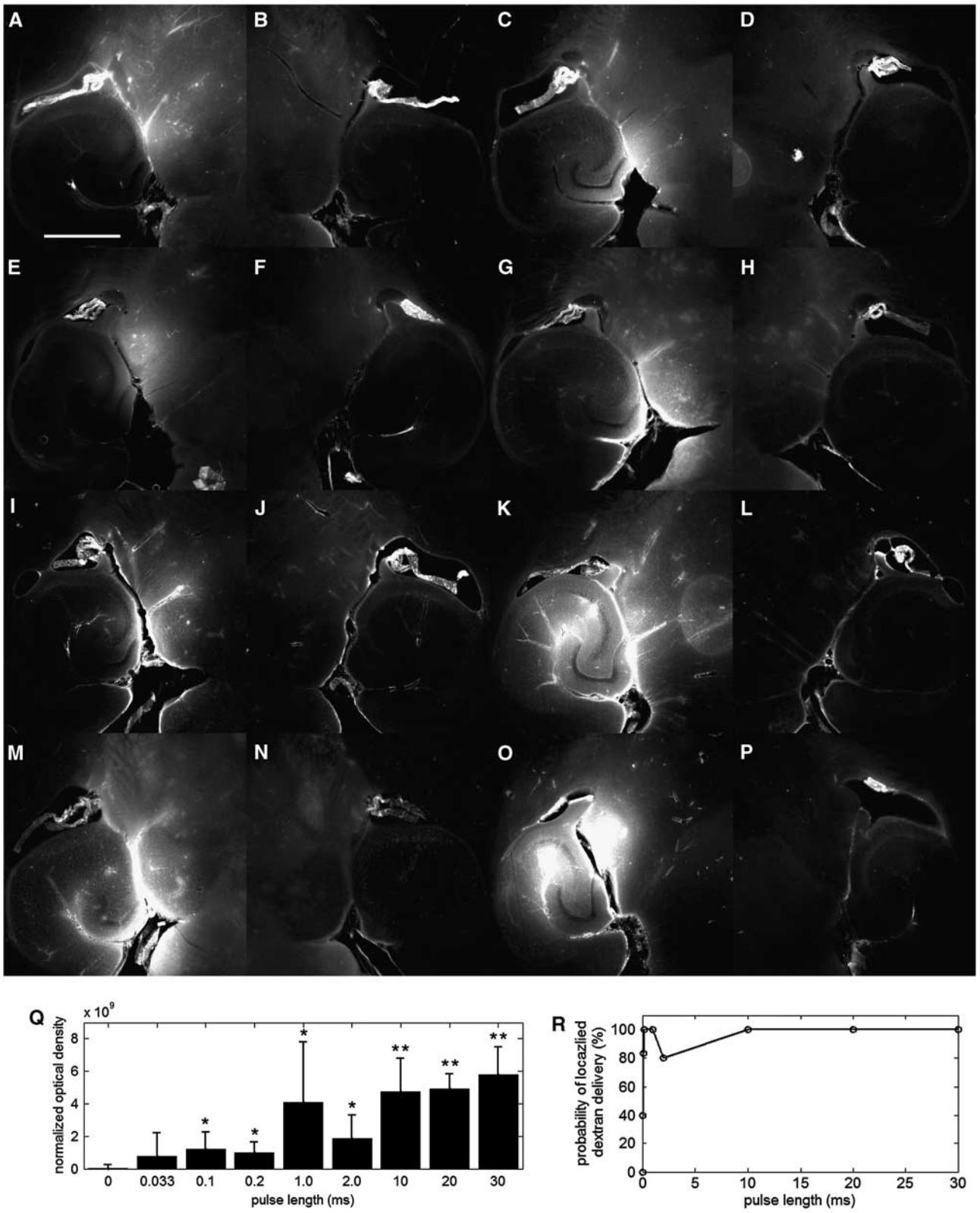

Figure 4 Qualitative fluorescence images of the (**A**, **C**, **E**, **G**, **I**, **K**, **M**, **O**) left and (**B**, **D**, **F**, **H**, **J**, **L**, **N**, **P**) right brain regions of interest (ROI) that have been exposed to pulse length (PL) of (**A**) 0.033, (**C**) 0.1, (**E**) 0.2, (**G**) 1, (**I**) 2, (**K**) 10, (**M**) 20, and (**O**) 30 milliseconds. The white scale bar in (**A**) indicates 1 mm. Quantitative (**Q**) normalized optical density (NOD) of the left focused ultrasound (FUS)-targeted ROI and (**R**) probability of localized dextran delivery. The left ROI was sonicated at different PLs. The single asterisk (*) indicates an NOD increase from the sham, whereas the double asterisk (**) indicates a significant increase compared with the 0.033-, 0.1-, and 0.2-millisecond PLs ($P < 0.05$).

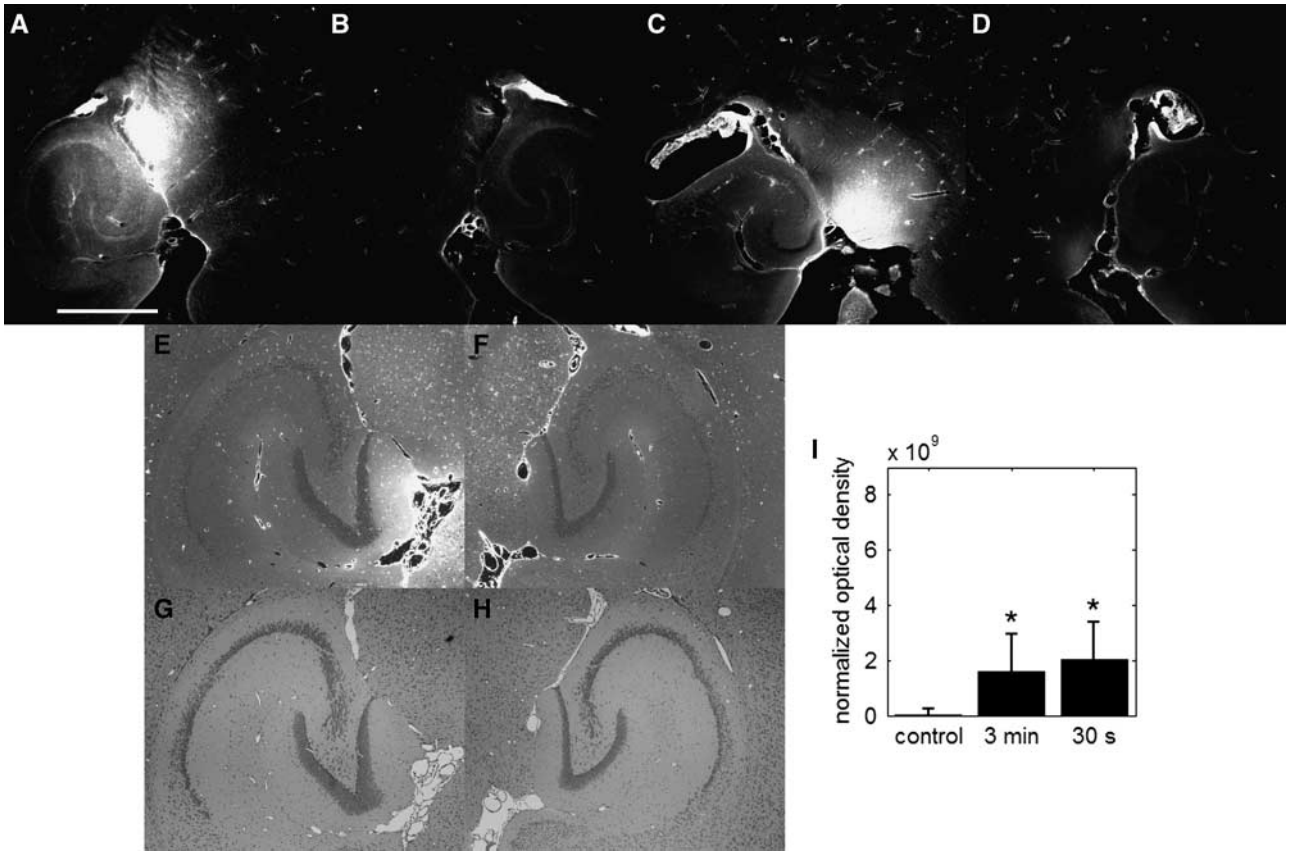

Figure 5 Qualitative fluorescence images of the (**A**, **C**, **E**, **G**) left and (**B**, **D**, **F**, **H**) right brain regions of interest (ROI) that have been exposed to a pulse length (PL) of 0.2 milliseconds at a pulse repetition frequency (PRF) of 5 Hz. (**A**) One of the mice was sonicated with a 3-minute microbubble injection time, whereas the (**C**) other was sonicated with a 30-second injection time. The white scale bar in (**A**) indicates 1 mm. The localization of fluorescent-tagged dextran was also observed in (**E**, **F**) unstained paraffin-embedded sections, which were analyzed with respect to its immediate neighboring sections that was (**G**, **H**) stained with hematoxylin and eosin. (**I**) Quantitative normalized optical density (NOD) of the left focused ultrasound (FUS)-targeted ROI. Both injection durations had NOD levels significantly greater than the sham as indicated by the asterisk (*) ($P < 0.05$).

insignificant despite the twofold increase in PL (Figure 4Q). The NOD at PLs of 10, 20, and 30 milliseconds were significantly higher than at 0.1 and 0.2 milliseconds, thus indicating increased dextran delivery. Finally, no significant difference was observed among PLs of 10, 20, and 30 milliseconds; thus indicating the possibility of limited increase of trans-BBB efficacy beyond a certain PL.

Acoustic Parameters near the Threshold of Blood–Brain Barrier Disruption

Dextran delivery was evaluated at a PL of 0.2 milliseconds and PRF of 5 Hz with Definity microbubbles injected over 30 or 180 seconds (Figures 5A and 5C). Significant NOD increase and dextran delivery were observed in all mice (10 out of 10) (Figure 5I). The dextran was diffusely distributed throughout the targeted region, and containment within or near large vessels was mostly avoided. No significant difference was observed between the 30- and 180-seconds microbubble injection durations.

In the case of the 180-second injection duration, brains were microscopically examined for damage. Fluorescence increase because of dextran delivery was observed in the sonicated ROI of the paraffin-embedded sections (Figure 5E) compared with the control ROI (Figure 5F). The immediate neighboring sections were stained with H&E (Figures 5G and 5H), and no dark neurons, microvacuolations, or erythrocyte extravasation sites were observed. The total number of dark neurons, microvacuolations, and erythrocyte extravasation sites in the left hemisphere relative to the right were quantified to be -24.0 ± 13.1, 0.2 ± 0.4, and 0.8 ± 2.2, thus showing no significant difference compared with the control, which corresponded to 4.33 ± 8.39, 0 ± 0, and 0.3 ± 0.58, respectively.

Discussion

This study investigated a wide range of ultrasound and microbubble conditions that may induce BBB disruption. Parameters that have been previously

used by our group and others (PLs of $\geqslant$10 milliseconds and PRFs of 1 or 10 Hz) were determined not to be critical and essential for BBB disruption. Instead, we expected BBB disruption to be correlated with the number of acoustic cycles that the brain is exposed to, while the microbubbles perfuse the microvasculature. As a result, several experimental conditions were explored including sonication duration, microbubble concentration, PRF, and PL as detailed below.

Sonication Duration

Two protocols consisting of distinct sequences and durations of tracer injection, microbubble injection, and sonication consistently delivered dextran to the target ROI. Ultrasound was transmitted for either 30 seconds or 11 minutes, and each had a distinct protocol. Despite the 22-fold increase in sonication duration from 30 seconds to 11 minutes, there was no significant difference in the delivered concentration or spatial distribution (Figure 2). Either increasing the total number of emitted acoustic cycles (i.e., longer acoustic exposure durations) does not correspond to increased concentrations of dextran delivered or, with the 30-second sonication, the maximal efficacy was already reached within this duration. However, this lack of increase may not hold for all ultrasound and microbubble conditions, as we evaluated protocol dependencies using a distinct set of PRFs, PLs, and acoustic pressures.

Microbubble Concentration

Sonication with microbubbles at concentrations of 0.01, 0.05, and 0.25 μL/g consistently increased cerebrovascular permeability. However, different concentrations of dextran delivered did not produce statistically significant changes. Our results agree with a previous study that used a similar range of acoustic pressures and microbubble concentrations (McDannold *et al*, 2008). Our hypothesis was that if microbubble-induced mechanical stress on the BBB is required to disrupt it, as previous studies have suggested (Choi *et al*, 2010*a*; Raymond *et al*, 2007), then more acoustically activated bubbles would generate more sites of increased permeability within the vasculature, and therefore, deliver a larger concentration of agents. In fact, another group has shown a dependence of FUS-induced BBB disruption on microbubble concentration (Yang *et al*, 2007). However, in that study, different ultrasound and microbubble conditions were used including a higher peak-rarefactional pressure (0.9 and 1.2 MPa) than what was studied here. Thus, the microbubble concentration may still constitute an influential parameter, but it was not shown to be significantly important at the specific ultrasound and microbubble conditions evaluated in this study.

Pulse Repetition Frequency

Several key findings on the PRF were reported. First, a minimum number of pulses is required to induce BBB disruption. If microbubbles are assumed to persist in circulation for 5 minutes (Sirsi *et al*, 2010), then an estimated 30 pulses at a 0.1-Hz PRF is insufficient in disrupting the BBB. Second, a 1-Hz PRF inconsistently disrupted the BBB and, when it did, both the delivered dextran concentration and spatial distribution greatly varied. One possible explanation for this variability stems from the need of microbubbles to be distributed throughout the microvessels as no BBB exists in larger vessels. Sonication causes microbubbles to destruct (e.g., inertial cavitation, fragmentation) or change in shape and size (e.g., rectified diffusion, ripening) (Apfel, 1997; Borden *et al*, 2005; Chomas *et al*, 2001). If each pulse destroys or modifies a portion of microbubbles in a way that reduces their ability to increase cerebrovascular permeability, then a long time interval between pulses may be necessary to replenish the microvessels. This was previously observed for the specific purpose of acoustically induced microbubble fragmentation (Samuel *et al*, 2009). Thus, the large variations observed at 1 Hz may be caused by competing effects of sufficient microbubble reperfusion of the microvasculature and acoustic exposure. As large vessels have a higher blood velocity than capillaries, the consistent fluorescence increase at PRFs of 5, 10, and 25 Hz may be due to not only BBB disruption occurring during the first few pulses, but also microbubble-induced dextran accumulation at or near the larger vessels during subsequent pulses. Further studies are warranted to further examine reperfusion effects. Finally, NOD levels at PRFs of 5, 10, and 25 Hz were not significantly different among each other. This lack of increase with increasing exposure may be due to subsequent pulses at high PRFs, which disturb the normal microbubble microvascular reperfusion. Another reason might be that an increase of the PRF simply 'saturates' the number of possibly disrupted sites along the vessels and that maximal dextran delivery has been reached at 5 Hz.

Pulse Length

To our knowledge, our study investigated a wider range of PLs *in vivo* than any previous study reported, and several interesting results were found. First, we induced BBB disruption at a 33-microsecond (50 cycles) PL. This was recorded in two out of five mice (40%) and is the lowest reported PL shown feasible to locally deliver agents in the brain at low acoustic pressures ($<$0.5 MPa peak rarefactional). A previous study showed that BBB disruption could occur at 10 microseconds, but required a high pressure of 6.3 MPa (Hynynen *et al*, 2003). Thus, our finding goes against the previously existent notion that long PLs are necessary for BBB

disruption to occur at low acoustic pressures. Second, sonication with a 0.1-millisecond PL exhibited greater consistency of BBB disruption (5 out of 6 mice or 83%) than previously reported (McDannold *et al*, 2008). This previous study used the same 0.1-millisecond PL, but at a 1-Hz PRF for 20 seconds using a 0.69-MHz transducer and resulted in lower probabilities of 20% and 17% at 0.4 and 0.5 MPa, respectively (McDannold *et al*, 2008). The lower probability may be due to one or more of the many differences between our study designs including our longer, 11-minutes sonication duration. Third, BBB disruption was consistently induced at a 0.2-millisecond PL, and, to our knowledge, this is the lowest PL reported to have accomplished this (5 out of 5 mice or 100%). Beyond PLs of 0.2 milliseconds (1, 10, 20, and 30 milliseconds), consistent delivery was produced except at 2 milliseconds, which had a deviation (1 out of 5 mice did not exhibit detectable levels of dextran). Regardless, these PLs significantly increased the concentration of dextran delivered (Figure 4). Finally, there appears to be a plateau effect beyond a PL of 10 milliseconds. At a PL of 10, 20, and 30 milliseconds, the increase in delivered concentrations was significantly greater than at 0.033, 0.1, and 0.2 millisecond PLs (Figure 4). Our results are in good agreement with a prior finding where a significant increase in the concentration of an MR contrast agent was observed from 0.1 to 10 milliseconds (McDannold *et al*, 2008). Also, no significant difference was observed between 10, 20, and 30 milliseconds, thus also showing good agreement with what has been previously reported, i.e., no increase in efficacy was observed with PLs >10 milliseconds (Hynynen *et al*, 2001).

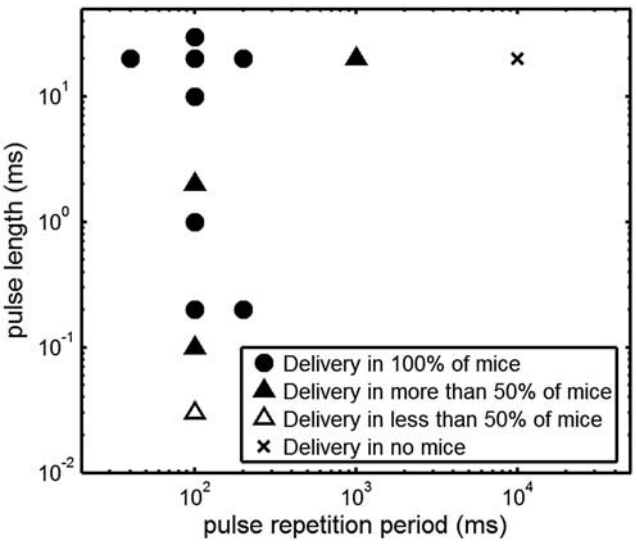

Figure 6 The design space of acoustic conditions shown to induce localized delivery of 3-kDa dextran. Sonications were applied for 11 minutes at a peak-rarefactional pressure of 0.46 MPa and with a 30-second intravenous bolus of microbubbles of 0.05 μL/g of body mass.

Generation and Avoidance of Blood–Brain Barrier Disruption

The broad finding from this study was that a wider range of acoustic and microbubble conditions may be used to induce BBB disruption than was previously thought. In the case of brain drug delivery, this allows greater freedom in designing an optimal set of protocols and parameters (Figure 6). Indeed, lower PLs and PRFs may result in a more homogenous spatial distribution of 3-kDa dextran in the targeted brain region (Figure 5) and was also confirmed relative to our previous work with 3-kDa dextran (Choi *et al*, 2010*b*), where we used a longer PL, higher PRF, and slightly higher peak-rarefactional pressure (PL: 20 milliseconds, PRF: 10 Hz, sonication duration: 1 minute, center frequency: 1.525 MHz, pressure: 0.57 MPa). The previous paper also suggested that the accumulation of 3-kDa dextran near larger vessels may correlate with the heterogeneous distribution of 70-kDa dextran. However, determining whether a better distribution of 70-kDa dextran can be achieved with lower PLs and PRFs remains to be shown and is part of our ongoing studies. Regardless, our low PL and PRF parameters were indicated as safe according to our assessment using H&E staining (Figure 5). No significant increase in dark neurons, microvacuolations, and erythrocyte extravasation sites were observed.

In cases where increased cerebrovascular permeability should be avoided (e.g., sonothrombolysis and cerebral blood flow imaging), the range of acoustic parameters are further constrained to shorter PLs (<33 microseconds) and reduced PRFs (<1 Hz). Our results had several differences than those reported in McDannold *et al* (2008). One of the key differences was that we used a longer (11 minutes) sonication duration as opposed to their 20 seconds sonication duration. Although our investigation at a PRF 10 Hz and a PL of 20 milliseconds showed that this sonication duration difference did not produce significant difference in NOD, it may still be the cause for varying results at lower PRFs and PLs. If this is the case, then a necessary principle for inducing BBB disruption may be a sufficient period of ultrasound–microbubble interaction with the microvasculature. Thus, inducing or avoiding BBB disruption may entail the careful selection of this duration. We plan on testing this hypothesis in future experiments.

Another key parameter necessary for BBB disruption is the peak-rarefactional pressure, which was 0.46 MPa in this study. Previously, our group showed that, at 0.46 MPa, a broadband response, which is an indicator of inertial cavitation activity, was detected *in vivo* and through the mouse skull (Tung *et al*, 2010). This infers that inertial cavitation was present and may be responsible for the BBB disruption observed in our results. However, BBB disruption

at lower pressures (e.g., 0.3 MPa) has been demonstrated in previous reports (Choi *et al*, 2010*a*; Tung *et al*, 2010) and disruption may still be achieved using low PLs and without inertial cavitation.

This study was possible in large part because of the high-throughput *in vivo* brain targeting system we have developed. The system's performance was described previously (Choi *et al*, 2007*a*, *b*) and observed in Figures 2–6. Despite the accuracy of the targeting, the lateral dimension of the FUS beam is ~1.3 mm in diameter and is bound to experience some variability among different mice. For example, in the case shown in Figures 2I and 2J, the system may have been off-target as an increase in fluorescence was observed in the choroid plexus, and this may have introduced some error in our NOD calculation. However, this was a rare occasion and was the only brain where fluorescence increases in the left choroid plexus were observed relative to the right. In the same mouse, only three of the nine sections analyzed had this fluorescence. Regardless, fluorescence in the choroid plexus may be of importance and will be investigated in future studies.

Clinical Implications

One of the primary concerns with noninvasive FUS sonication in the human brain is the need to decrease the acoustic frequency to allow for efficient transcranial transmission of the ultrasonic wave (Hynynen *et al*, 2006). However, long PLs of 500 microseconds at a low frequency of 300 kHz have been shown to generate standing waves and may be a cause for the onset of hemorrhage during clinical trial of sonothrombolysis (Baron *et al*, 2009; Tsivgoulis and Alexandrov, 2007). Our results are particularly interesting, because we have shown that BBB disruption can occur at extremely low PLs (i.e., 33 microseconds), thus allowing for the possibility of reducing or avoiding standing wave effects.

Conclusions

This study has identified a larger and more descriptive design space of ultrasound and microbubble conditions that increase cerebrovascular permeability than was previously reported. We have shown that two protocols, with either a 30-second or 11-minute sonication duration, and three microbubble concentrations of 0.01, 0.05, and 0.25 μL/g could all disrupt the BBB. The lowest PRF at which disruption was feasible was 1 Hz, whereas the lowest PRF at which disruption was consistently produced was 5 Hz. The lowest PL at which disruption was feasible was 0.033 milliseconds, whereas the lowest PL at which disruption was consistently produced was 0.2 milliseconds. To our knowledge, these PLs are the lowest reported in the literature, thus disproving the notion that long PLs are necessary for BBB disruption to occur. Short PLs may also allow for reduction or complete elimination of standing wave effects in the human skull. Finally, the lowest PL and PRF that consistently led to dextran delivery (PRF: 5 Hz, PL: 0.2 milliseconds) were combined to consistently induce BBB disruption and deliver a diffuse distribution of dextran without any associated concentrations within or near large vessels. The safety of this parameter was confirmed under H&E histology. These findings have collectively demonstrated that a unique set of ultrasonic pulses and microbubble conditions may be generated noninvasively and locally in a deep subcortical structure to deliver a uniform distribution of drugs across the BBB.

Acknowledgements

The authors thank the Riverside Research Institute (New York, NY, USA) for providing the transducers; Thomas Deffieux for discussions on the selection of the acoustic and microbubble conditions to explore, and on the calculation of the NOD; and Mark Borden and Shashank Sirsi for discussions concerning the microbubble persistence timeline.

Disclosure/conflict of interest

The authors declare no conflict of interest.

References

Apfel RE (1997) Sonic effervescence: a tutorial on acoustic cavitation. *J Acoust Soc Am* 101:1227–37

Baron C, Aubry JF, Tanter M, Meairs S, Fink M (2009) Simulation of intracranial acoustic fields in clinical trials of sonothrombolysis. *Ultrasound Med Biol* 35:1148–58

Baseri B, Choi JJ, Tung YS, Konofagou EE (2010) Multi-modality safety assessment of blood-brain barrier opening using focused ultrasound and definity microbubbles: a short-term study. *Ultrasound Med Biol* 36:1445–59

Borden MA, Kruse DE, Caskey CF, Zhao S, Dayton PA, Ferrara KW (2005) Influence of lipid shell physicochemical properties on ultrasound-induced microbubble destruction. *IEEE Trans Ultrason Ferroelectr Freq Control* 52:1992–2002

Cammermeyer J (1960) The post-mortem origin and mechanism of neuronal hyperchromatosis and nuclear pyknosis. *Exp Neurol* 2:379–405

Cammermeyer J (1978) Is the solitary dark neuron a manifestation of postmortem trauma to the brain inadequately fixed by perfusion? *Histochemistry* 56:97–115

Choi JJ, Pernot M, Brown TR, Small SA, Konofagou EE (2007*a*) Spatio-temporal analysis of molecular delivery through the blood-brain barrier using focused ultrasound. *Phys Med Biol* 52:5509–30

Choi JJ, Pernot M, Small SA, Konofagou EE (2007*b*) Noninvasive, transcranial and localized opening of the blood-brain barrier using focused ultrasound in mice. *Ultrasound Med Biol* 33:95–104

Choi JJ, Feshitan JA, Baseri B, Wang S, Tung YS, Borden MA, Konofagou EE (2010*a*) Microbubble-size dependence

of focused ultrasound-induced blood-brain barrier opening in mice *in vivo*. *IEEE Trans Biomed Eng* 57:145–54

Choi JJ, Wang S, Tung YS, Morrison III B, Konofagou EE (2010*b*) Molecules of various pharmacologically-relevant sizes can cross the ultrasound-induced blood-brain barrier opening in vivo. *Ultrasound Med Biol* 36:58–67

Chomas JE, Dayton P, May D, Ferrara K (2001) Threshold of fragmentation for ultrasonic contrast agents. *J Biomed Opt* 6:141–50

Datta S, Coussios CC, Ammi AY, Mast TD, de Courten-Myers GM, Holland CK (2008) Ultrasound-enhanced thrombolysis using Definity as a cavitation nucleation agent. *Ultrasound Med Biol* 34:1421–33

Hynynen K, McDannold N, Martin H, Jolesz FA, Vykhodtseva N (2003) The threshold for brain damage in rabbits induced by bursts of ultrasound in the presence of an ultrasound contrast agent (Optison). *Ultrasound Med Biol* 29:473–81

Hynynen K, McDannold N, Vykhodtseva N, Jolesz FA (2001) Noninvasive MR imaging-guided focal opening of the blood-brain barrier in rabbits. *Radiology* 220:640–6

Hynynen K, McDannold N, Vykhodtseva N, Raymond S, Weissleder R, Jolesz FA, Sheikov N (2006) Focal disruption of the blood-brain barrier due to 260-kHz ultrasound bursts: a method for molecular imaging and targeted drug delivery. *J Neurosurg* 105:445–54

Kinoshita M, McDannold N, Jolesz FA, Hynynen K (2006) Noninvasive localized delivery of Herceptin to the mouse brain by MRI-guided focused ultrasound-induced blood-brain barrier disruption. *Proc Natl Acad Sci USA* 103:11719–23

McDannold N, Vykhodtseva N, Hynynen K (2008) Effects of acoustic parameters and ultrasound contrast agent dose on focused-ultrasound induced blood-brain barrier disruption. *Ultrasound Med Biol* 34:930–7

Meairs S, Culp W (2009) Microbubbles for thrombolysis of acute ischemic stroke. *Cerebrovasc Dis* 27(Suppl 2): 55–65

Meyer-Wiethe K, Sallustio F, Kern R (2009) Diagnosis of intracerebral hemorrhage with transcranial ultrasound. *Cerebrovasc Dis* 27(Suppl 2):40–7

Raymond SB, Skoch J, Hynynen K, Bacskai BJ (2007) Multiphoton imaging of ultrasound/Optison mediated cerebrovascular effects *in vivo*. *J Cereb Blood Flow Metab* 27:393–403

Samuel S, Cooper MA, Bull JL, Fowlkes JB, Miller DL (2009) An ex vivo study of the correlation between acoustic emission and microvascular damage. *Ultrasound Med Biol* 35:1574–86

Sirsi S, Feshitan J, Kwan J, Homma S, Borden M (2010) Effect of microbubble size on fundamental mode high frequency ultrasound imaging in mice. *Ultrasound Med Biol* 36:935–48

Treat LH, McDannold N, Vykhodtseva N, Zhang Y, Tam K, Hynynen K (2007) Targeted delivery of doxorubicin to the rat brain at therapeutic levels using MRI-guided focused ultrasound. *Int J Cancer* 121:901–7

Tsivgoulis G, Alexandrov AV (2007) Ultrasound-enhanced thrombolysis in acute ischemic stroke: potential, failures, and safety. *Neurotherapeutics* 4:420–7

Tsivgoulis G, Alexandrov AV, Sloan MA (2009) Advances in transcranial Doppler ultrasonography. *Curr Neurol Neurosci Rep* 9:46–54

Tung YS, Choi JJ, Baseri B, Konofagou EE (2010) Identifying the inertial cavitation threshold and skull effects in a vessel phantom using focused ultrasound and microbubbles. *Ultrasound Med Biol* 36:840–52

Yang FY, Fu WM, Yang RS, Liou HC, Kang KH, Lin WL (2007) Quantitative evaluation of focused ultrasound with a contrast agent on blood-brain barrier disruption. *Ultrasound Med Biol* 33:1421–7